



A tunable narrow-linewidth Raman laser based on high quality packaged microrod resonator

Cheng-Nian Liu(刘承念), Min Wang(王敏), Song-Yi Liu(刘嵩义), Bing Duan(段冰), Ying-Zhan Yan(严英占), Yu Wu(吴宇), Xiao-Chong Yu(俞骁翀), Bei-Bei Li(李贝贝), and Da-Quan Yang(杨大全)

Citation: Chin. Phys. B, 2025, 34 (12): 124203. DOI: 10.1088/1674-1056/adea5a

<http://cpb.iphy.ac.cn>; <http://iopscience.iop.org/cpb>

What follows is a list of articles you may be interested in

Gigahertz frequency hopping in an optical phase-locked loop for Raman lasers

Dekai Mao(毛德凯), Hongmian Shui(税鸿冕), Guoling Yin(殷国玲), Peng Peng(彭鹏), Chunwei Wang(王春唯), and Xiaoji Zhou(周小计)

Chin. Phys. B, 2024, 33 (2): 024209. DOI: 10.1088/1674-1056/ad174b

Multi-wavelength continuous-wave Nd:YVO₄ self-Raman laser under in-band pumping

Li Fan(樊莉), Xiao-Dong Zhao(赵孝冬), Yun-Chuan Zhang(张蕴川), Xiao-Dong Gu(顾晓东), Hao-Peng Wan(万浩鹏), Hui-Bo Fan(范会博), Jun Zhu(朱骏)

Chin. Phys. B, 2019, 28 (8): 084210. DOI: 10.1088/1674-1056/28/8/084210

High-power linearly-polarized tunable Raman fiber laser

Jiaxin Song(宋家鑫), Hanshuo Wu(吴函烁), Jiangming Xu(许将明), Hanwei Zhang(张汉伟), Jun Ye(叶俊), Jian Wu(吴坚), Pu Zhou(周朴)

Chin. Phys. B, 2018, 27 (9): 094209. DOI: 10.1088/1674-1056/27/9/094209

An efficient continuous-wave YVO₄/Nd: YVO₄/YVO₄ self-Raman laser pumped by a wavelength-locked 878.9 nm laser diode

Li Fan(樊莉), Weiqian Zhao(赵伟倩), Xin Qiao(乔鑫), Changquan Xia(夏长权), Lichun Wang(汪丽春), Huibo Fan(范会博), Mingya Shen(沈明亚)

Chin. Phys. B, 2016, 25 (11): 114207. DOI: 10.1088/1674-1056/25/11/114207

Backward Raman amplification in plasmas with chirped wideband pump and seed pulses

Wu Zhao-Hui(吴朝辉), Wei Xiao-Feng(魏晓峰), Zuo Yan-Lei(左言磊), Liu Lan-Qin(刘兰琴), Zhang Zhi-Meng(张智猛), Li Min(李敏), Zhou Yu-Liang(周煜梁), Su Jing-Qin(粟敬钦)

Chin. Phys. B, 2015, 24 (1): 014211. DOI: 10.1088/1674-1056/24/1/014211

CPB

Chinese Physics B

Volume 34 December 2025 Number 12

SPECIAL TOPIC

- Biophysical circuits: Modeling & applications in neuroscience
- Ultrafast physics in atomic, molecular and optical systems

A series Journal of the Chinese Physical Society Distributed by IOP Publishing

iopscience.org/cpb | cpb.iphy.ac.cn



Featured Article

MaterialsGalaxy: A platform fusing experimental and theoretical data in condensed matter Physics

Tiannian Zhu, Zhong Fang, Quansheng Wu, Hongming Weng

Chin. Phys. B, 2025, 34: 120702

Chinese Physics B (中国物理B)

First published in 1992. Published monthly in hard copy by the Chinese Physical Society and online by IOP Publishing, No. 2 The Distillery, Glassfields, Avon Street, Bristol BS2 0GR, UK

Institutional subscription information: 2025 volume

For all countries, except the United States, Canada and Central and South America, the subscription rate per annual volume is UK £1749 (electronic only).

Orders to:

Journals Subscription Fulfilment, IOP Publishing, No. 2 The Distillery, Glassfields, Avon Street, Bristol BS2 0GR, UK

For the United States, Canada and Central and South America, the subscription rate per annual volume is US\$3485 (electronic only).

Orders to: IOP Publishing, P. O. Box 320, Congers, NY 10920-0320, USA

© 2025 Chinese Physical Society and IOP Publishing Ltd

All rights reserved. No part of this publication may be reproduced, stored in a retrieval system, or transmitted in any form or by any means, electronic, mechanical, photocopying, recording or otherwise, without the prior written permission of the copyright owner.

Editorial Office: Institute of Physics, Chinese Academy of Sciences, P. O. Box 603, Beijing 100190, China

Tel: (86-10) 82649026 or 82649519, Fax: (86-10) 82649027, E-mail: cpb@aphy.iphy.ac.cn

主管单位: 中国科学院

国际统一刊号: ISSN 1674-1056

主办单位: 中国物理学会和中国科学院物理研究所

国内统一刊号: CN 11-5639/O4

编辑: Chinese Physics B 编辑部

编辑部地址: 北京 中关村 中国科学院物理研究所内

出版: 中国物理学会

通信地址: 100190 北京 603 信箱

出版日期: 2025年12月

电话: (010) 82649026, 82649519

印刷装订: 北京科信印刷有限公司

传真: (010) 82649027

国内发行: Chinese Physics B 编辑部

“Chinese Physics B”网址:

国外发行: IOP Publishing Ltd

<http://cpb.iphy.ac.cn>

发行范围: 公开发行

<http://iopscience.iop.org/journal/1674-1056>

Advisory Board

Chen Jia-Er(陈佳洱), Samuel C. C. Ting(丁肇中), Wang Nai-Yan(王乃彦),
Zhao Zhong-Xian(赵忠贤), Yang Guo-Zhen(杨国桢)

Editorial Board

Editor-in-Chief

Gao Hong-Jun(高鸿钧)

Chinese Academy of Sciences, China

Associate Editors

Chen Xian-Hui(陈仙辉)

University of Science and Technology of China, China

Fan Heng(范桁)

Institute of Physics, Chinese Academy of Sciences, China

Gao Yuan-Ning(高原宁)

Peking University, China

Li Jian-Xin(李建新)

Nanjing University, China

Li Ru-Xin(李儒新)

Shanghai Tech University, China

Ma Yan-Ming(马琰铭)

Jilin University, China

Ouyang Zhong-Can(欧阳钟灿)

Institute of Theoretical Physics, Chinese Academy of Sciences, China

Shen Bao-Gen(沈保根)	Institute of Physics, Chinese Academy of Sciences, China
Wang Wei-Hua(汪卫华)	Institute of Physics, Chinese Academy of Sciences, China
Wang Zi-Qiang(汪自强)	Boston College USA
Wang Ning(王宁)	The Hong Kong University of Science and Technology, China
Xiong Qi-Hua(熊启华)	Tsinghua University, China
Yao Wang(姚望)	The University of Hong Kong, China
Zhang Jie(张杰)	Chinese Physical Society, China
Zhang Yuan-Bo(张远波)	Fudan University, China

Editorial Board

Chen Chong-Lin(陈充林)	University of Texas at San Antonio, USA
Chen Wei(陈伟)	National University of Singapore, Singapore
Chen Xiao-Song(陈晓松)	Beijing Normal University, China
Chen Yu-Ao(陈宇翱)	University of Science and Technology of China, China
Cheng Jian-Chun(程建春)	Nanjing University, China
Cheng Meng(程蒙)	Yale University, USA
Cui Xiao-Dong(崔晓冬)	The University of Hong Kong, China
Dai Qing(戴庆)	National Center for Nanoscience and Technology, China
Dai Xi(戴希)	The Hong Kong University of Science and Technology, China
Ding Da-Jun(丁大军)	Jilin University, China
Fang Zhong(方忠)	Institute of Physics, Chinese Academy of Sciences, China
Feng Shi-Ping(冯世平)	Beijing Normal University, China
Feng Xin-Liang(冯新亮)	Dresden University of Technology, Germany
Gao Wei-Bo(高伟博)	Nanyang Technological University, Singapore
Gong Xin-Gao(龚新高)	Fudan University, China
Gu Chang-Zhi(顾长志)	Institute of Physics, Chinese Academy of Sciences, China
Guo Hong(郭鸿)	McGill University, Canada
Hu Xiao(胡晓)	National Institute for Materials Science, Japan
Huang Xue-Jie(黄学杰)	Institute of Physics, Chinese Academy of Sciences, China
Ji Wei(季威)	Renmin University of China, China
Jia Jin-Feng(贾金锋)	Shanghai Jiao Tong University, China
Jiang Ying(江颖)	Peking University, China
Leong Chuan Kwek	National University of Singapore, Singapore
Lei Danguan(雷党愿)	City University of Hong Kong, China
Li Bao-Wen(李保文)	Southern University of Science and Technology, China
Li Jian-Qi(李建奇)	Institute of Physics, Chinese Academy of Sciences, China
Li Xiao-Guang(李晓光)	University of Science and Technology of China, China
Liu Bing-Bing(刘冰冰)	Jilin University, China
Liu Chao-Xing(刘朝星)	Pennsylvania State University, USA
Liu Xiang-Yang(刘向阳)	Xiamen University, China
Liu Yi-Chun(刘益春)	Northeast Normal University, China
Liu Zheng(刘政)	Nanyang Technological University, Singapore
Long Gui-Lu(龙桂鲁)	Tsinghua University, China
Lu Zheng-Tian(卢征天)	University of Science and Technology of China, China
Lu Wei(陆卫)	Shanghai Institute of Technical Physics, Chinese Academy of Sciences, China
Luo Hong-Gang(罗洪刚)	Lanzhou University, China
Lu Guang-Hong(吕广宏)	Beihang University, China
Lu Li(吕力)	Institute of Physics, Chinese Academy of Sciences, China

Ma Xu-Cun(马旭村)	Tsinghua University, China
Ma Yu-Gang(马余刚)	Fudan University, China
Ni Pei-Gen(倪培根)	National Natural Science Foundation of China, China
Niu Qian(牛谦)	University of Texas, USA
Ouyang Qi(欧阳颀)	Zhejiang University, China
Pan Yi(潘毅)	Xi'an Jiaotong University, China
Shen De-Zhen(申德振)	Changchun Institute of Optics, Fine Mechanics and Physics, Chinese Academy of Sciences, China
Shen Ze-Xiang(申泽骧)	Nanyang Technological University, Singapore
Shen Jian(沈健)	Fudan University, China
Si Qi-Miao(斯其苗)	Rice University, USA
Sun Chang-Pu(孙昌璞)	Beijing Computational Science Research Center, China
Sun Xiao Wei(孙小卫)	Southern University of Science and Technology, China
Tian Yong-Jun(田永君)	Yanshan University, China
Tong Li-Min(童利民)	Zhejiang University, China
John S. Tse	University of Saskatchewan, Canada
Wan Bao-Nian(万宝年)	Institute of Plasma Physics, Chinese Academy of Sciences, China
Wang Bo-Gen(王伯根)	Nanjing University, China
Wang Kai-You(王开友)	Institute of Semiconductors, Chinese Academy of Sciences, China
Wang Wei(王炜)	Nanjing University, China
Wang Ya-Yu(王亚愚)	Tsinghua University, China
Wang Yu-Peng(王玉鹏)	Institute of Physics, Chinese Academy of Sciences, China
Wei Su-Huai(魏苏淮)	Eastern Institute of Technology, Ningbo, China
Wen Wei-Jia(温维佳)	The Hong Kong University of Science and Technology, China
Wen Hai-Hu(闻海虎)	Nanjing University, China
Wu Nan-Jian(吴南健)	Institute of Semiconductors, Chinese Academy of Sciences, China
Xiang Tao(向涛)	Institute of Physics, Chinese Academy of Sciences, China
Xie Xin-Cheng(谢心澄)	Peking University, China
Xu Hong-Xing(徐红星)	Wuhan University, China
Xu Zhi-Chuan(徐志川)	Nanyang Technological University, Singapore
Yang Guo-Wei(杨国伟)	Sun Yat-Sen University, China
Yang Lan(杨兰)	Washington University in St. Louis, USA
Ye Jun(叶军)	University of Colorado, USA
Zhang Fu-Chun(张富春)	University of Chinese Academy of Sciences, China
Zhang Hong(张红)	Sichuan University, China
Zhang Yong(张勇)	The University of North Carolina at Charlotte, USA
Zhang Zhen-Yu(张振宇)	University of Science and Technology of China, China
Zhao Hong-Wei(赵红卫)	Institute of Modern Physics, Chinese Academy of Sciences, China
Zhao Hui(赵辉)	The University of Kansas, USA
Zhao Wei-Juan(赵维娟)	Zhengzhou University, China
Zheng Zhi-Gang(郑志刚)	Huaqiao University, China
Zhou Wu(周武)	University of Chinese Academy of Sciences, China
Zhou Xin(周昕)	University of Chinese Academy of Sciences, China
Zhou Xin(周欣)	Wuhan Institute of Physics and Mathematics, Chinese Academy of Sciences, China
Zhou Xing-Jiang(周兴江)	Institute of Physics, Chinese Academy of Sciences, China
Zhu Bang-Fen(朱邦芬)	Tsinghua University, China

Editorial Staff

Wang Jiu-Li(王久丽) (Editorial Director) Cai Jian-Wei(蔡建伟) Zhai Zhen(翟振)

A tunable narrow-linewidth Raman laser based on high quality packaged microrod resonator

Cheng-Nian Liu(刘承念)^{1,2}, Min Wang(王敏)³, Song-Yi Liu(刘嵩义)^{1,2}, Bing Duan(段冰)^{1,2},
Ying-Zhan Yan(严英占)⁴, Yu Wu(吴宇)⁵, Xiao-Chong Yu(俞骁翀)^{6,7,†},
Bei-Bei Li(李贝贝)^{3,‡}, and Da-Quan Yang(杨大全)^{1,2,§}

¹State Key Laboratory of Information Photonics and Optical Communications,
Beijing University of Posts and Telecommunications, Beijing 100876, China

²School of Information and Communication Engineering, Beijing University of Posts and Telecommunications, Beijing 100876, China

³Beijing National Laboratory for Condensed Matter Physics, Institute of Physics, Chinese Academy of Sciences, Beijing 100190, China

⁴Information Science Research Institute, China Electronics Technology Group Corporation, Beijing 100876, China

⁵The Key Laboratory of Optical Fiber Sensing and Communications (Education Ministry of China),
University of Electronic Science and Technology of China, Chengdu 610054, China

⁶Department of Physics and Applied Optics Beijing Area Major Laboratory, Beijing Normal University, Beijing 100875, China

⁷School of Physics and Astronomy, Applied Optics Beijing Area Major Laboratory,
Key Laboratory of Multiscale Spin Physics, Ministry of Education, Beijing Normal University, Beijing 100875, China

(Received 28 April 2025; revised manuscript received 16 June 2025; accepted manuscript online 1 July 2025)

The enhancement of the microcavity quality factor contributes to fundamental linewidth reduction in microcavity lasers. This study demonstrates silica microrod resonators with quality factors approaching 10^9 , fabricated by CO₂ laser reflow technology. To improve practical applicability, low-loss package techniques were developed, yielding packaged resonators with optimized optical performance. Using this platform, stimulated Raman lasing was achieved with a pump mode Q -factor of 1.333×10^9 , exhibiting a threshold of 0.765 mW. The laser output stability was characterized by a standard deviation of 0.671 mV over 45 minutes of operation, with corresponding Allan deviation analysis. At the maximum output power of 106.4 μ W, the measured frequency noise spectral density reached 0.46 Hz²/Hz, corresponding to a linewidth of 2.89 Hz. Thermal tuning of the packaged module achieved a wavelength shift of 0.206 nm, with a temperature sensitivity of 8.92 pm/°C. This work establishes a new technical pathway for developing compact narrow-linewidth lasers, showing significant potential for medical diagnostics, optical communications, and defense applications.

Keywords: Raman laser, resonator, nonlinear optics, optical elements and devices

PACS: 42.55.-f, 42.60.Da, 42.65.-k, 42.79.-e

DOI: 10.1088/1674-1056/adea5a

CSTR: 32038.14.CPB.adea5a

1. Introduction

Narrow-linewidth lasers, owing to their low phase noise and long coherence length, play a critical role in cutting-edge applications such as coherent optical communication, quantum communication, precision metrology, gravitational wave detection, and high-resolution imaging.^[1–5] Whispering gallery mode (WGM) optical microcavities, characterized by their high quality (Q) factor and small mode volume, have emerged as ideal optical platforms for realizing low-threshold and narrow-linewidth lasers.^[6]

In general, increasing the quality factor of a microcavity resonator can significantly reduce the Schawlow–Townes (ST) linewidth of the laser.^[7] However, conventional microcavity lasers typically achieve lasing by integrating specific gain materials, such as rare-earth ions, organic dyes, or quantum dots, with silica microresonators.^[8–11] For instance, in 2003, Vahala

demonstrated laser emission at 1540 nm from a silica microsphere coated with an Er³⁺-doped sol–gel thin film.^[12] Later, Fan improved the doping process of rare-earth ions in the sol–gel method, successfully fabricating an Er³⁺-doped silica microbubble cavity with a Q -factor as high as 5.2×10^7 . They also achieved a tuning range of 4.4 nm through an all-optical tuning mechanism.^[13] Although this approach enhances the Q -factor of doped microcavities, it remains at least an order of magnitude lower than that of undoped counterparts, which hinders further narrowing of the laser linewidth.

Microcavity lasers based on nonlinear optical effects offer a promising alternative to circumvent this limitation. Stimulated Raman scattering (SRS) and stimulated Brillouin scattering (SBS) are representative third-order nonlinear effects. SRS arises from the interaction between pump photons and optical phonons, while SBS involves interactions between pump photons and acoustic phonons.^[14,15] Com-

[†]Corresponding author. E-mail: ydq@bupt.edu.cn

[‡]Corresponding author. E-mail: libeibei@iphy.ac.cn

[§]Corresponding author. E-mail: yuxc@bnu.edu.cn

© 2025 Chinese Physical Society and IOP Publishing Ltd. All rights, including for text and data mining, AI training, and similar technologies, are reserved.

<http://iopscience.iop.org/cpb> <http://cpb.iphy.ac.cn>

pared to SBS, SRS generates Stokes light with a larger frequency shift, which helps extend the wavelength range of existing light sources.^[16] To date, researchers have realized stimulated Brillouin lasers (SBLs) with sub-Hertz fundamental linewidths in silicon nitride microcavities,^[17–19] silica microtoroid resonators,^[19] silica microdisk resonators,^[21,22] and silica microrod resonators.^[23] In contrast, narrow-linewidth stimulated Raman lasers (SRLs) based on high- Q WGM microcavities have been rarely reported. For example, Lu achieved a Raman laser with a linewidth of 3 Hz in an SiO₂ microtoroid resonator.^[24] Bao demonstrated a Raman laser in a crystalline AlN-on-sapphire microcavity with a Q -factor of 3.6×10^6 . This laser exhibited a threshold of 8.3 mW and a frequency noise of 4.6 Hz²/Hz, corresponding to a linewidth of 29 Hz.^[25]

2. SRL linewidth theory

The fundamental linewidth of the SRL $\Delta\nu_{ST}$ can be described as follows:^[24,26]

$$\Delta\nu_{ST} = (1 + \alpha^2) \frac{2\pi(1 + K_Q)K_Q\hbar\nu^3}{PQ_0^2}, \quad (1)$$

Here, P denotes output power of the SRL, \hbar is the reduced Planck constant, ν is the SRL frequency, and α describes the phase fluctuation coupled from intra-cavity pump intensity fluctuation due to the Kerr nonlinearity. Moreover, Q_0 represents the intrinsic quality factor of the optical resonance mode associated with the SRL, while Q_e is the coupling-related quality factor. These parameters satisfy the relation $K_Q = Q_0/Q_e$. Equation (1) shows that the fundamental linewidth of the SRL is inversely proportional to the square of the microcavity Q -factor, implying that high- Q microcavities enable the generation of narrow-linewidth SRLs.

2.1. Fabrication

Figure 1(a) shows our automated system for fabricating silica microrod resonators through CO₂ laser reflow technology. The fabrication process utilizes a high-purity quartz preform rod with a diameter of 3 mm. Prior to processing, the preform rod is sectioned into predetermined lengths and rigidly mounted on a computer-controlled translational spindle using a mechanical chuck assembly. The spindle rotates at a constant angular velocity of 600 rpm to ensure uniform surface heating during laser micromachining. The CO₂ laser output power (maximum 75 W) is modulated by pulse-width modulation using an arbitrary function generator (AFG), while the duty cycle is adjusted through computer control. The laser beam is then focused through a ZnSe lens onto the preform rod. In the laser interaction zone, silica undergoes localized melting and ablation. Under surface tension, the molten material redistributes laterally, forming a groove structure.^[27] First,

bilateral grooves are fabricated by high-power (70% duty cycle) laser micromachining, constructing the foundational microcavity structure. Subsequently, the laser power is reduced to 30% duty cycle, and a stepper motor moves the preform rod at 2 mm/min, enabling bidirectional laser scanning between the grooves. This process will create a whispering gallery region with smooth surface and uniform roundness.^[28] Finally, multiple laser reflow cycles are performed at 20% duty cycle to achieve both surface quality enhancement and precise geometric control of the microcavity.

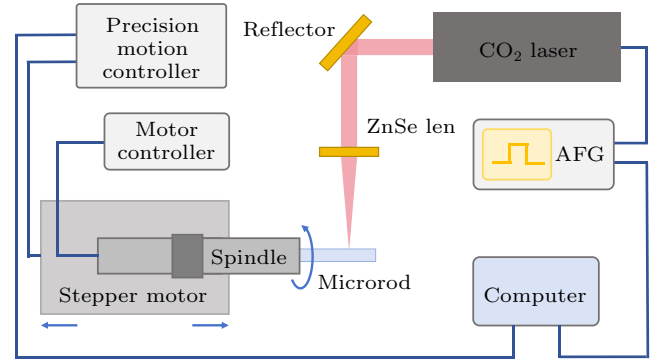


Fig. 1. The automated preparation system for silica microrod cavities. AFG: arbitrary function generator.

Figure 2(a) displays a fabricated silica microrod resonator. For optical characterization of the resonator, we statistically analyzed the quality-factor distribution of resonant modes within one free spectral range (FSR). As shown in Fig. 2(b), 21 resonant modes possess Q -factors above 10^9 , with the highest Q -factor reaching 2.3×10^9 . Furthermore, utilizing these optimized processing parameters in the automated fabrication setup enables reproducible production of microrod resonators with ultrahigh Q -factors.

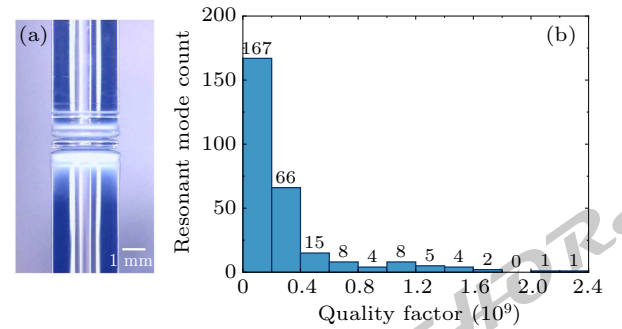


Fig. 2. Characterization of the microrod resonator: (a) optical microscope image of the microrod resonator, (b) Q -factor distribution of resonant modes within one FSR of the microrod resonator.

Despite their excellent optical performance, the practical application of microrod resonators faces significant challenges, including intricate coupling requirements, high sensitivity to environmental disturbances, and limited operational stability over extended periods. To address these issues, we developed a miniaturized and environmentally stable packaged resonator module. As illustrated in Fig. 3(a), the module features a dual-layer aluminum alloy architecture comprising inner and outer enclosures. The microrod resonator is fixed at

the central groove of the inner enclosure using UV-curable adhesive. The fiber taper, which couples to the microrod resonator, is also secured to the sidewalls of both the inner and outer enclosures using low-loss UV-curable adhesive. The thermal control system consists of a thermistor and a thermoelectric cooler (TEC). The gap between the inner and outer enclosure is filled with thermal conductive silicone, which enhances the mechanical stability of the module and facilitates efficient thermal transfer between the TEC and the inner enclosure. To further isolate the resonator from the external environment, the gaps between the sidewalls and the lid of the outer enclosure were sealed with UV-curable adhesive.

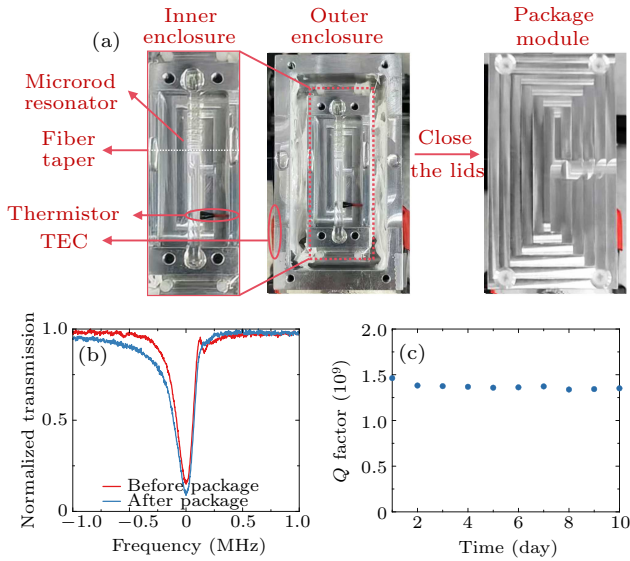


Fig. 3. Package module and performance characterization: (a) structural diagram of package module, (b) transmission spectrum of the same mode before and after packaging, (c) the Q -factor stability within 10 days.

Figure 3(b) presents the transmission spectrum of the same resonant mode acquired before and after packaging under the identical frequency-scanning rate. Prior to packaging, the resonant mode exhibited a narrower linewidth, along with an observable ringdown effect. To ensure accurate Q -factor measurements, the scanning speed was reduced to suppress the ringdown effect,^[29] yielding a calculated Q -factor of 1.507×10^9 . After packaging, the mode's linewidth broadened, and the ringdown phenomenon disappeared, resulting in a measured Q -factor of 1.445×10^9 . These results demonstrate that despite introducing additional optical losses during packaging, the encapsulated module retains a high Q -factor. The variation of the Q -factor in the packaged module over a 10-day period was measured, as shown in Fig. 3(c). A noticeable reduction in the Q -factor was observed on the second day after packaging, attributed to the adsorption of water molecules from ambient air onto the silica microcavity surface, which increased optical dissipation.^[30] Thereafter, the Q -factor stabilized, suggesting that the surface hydroxyl group may have reached saturation, allowing the packaged module to maintain a relatively stable Q -factor in the subsequent days.

2.2. Experiment

Figure 4 illustrates the experimental setup for SRL generation and characterization based on the packaged microrod resonator. The transmission signal from the microrod resonator is monitored by oscilloscope (OSC1) and fed back to a servo to achieve laser frequency locking.^[31] A Raman wavelength-division multiplexer (RWDM) separates and outputs laser signals at 1450 nm, 1550 nm, and 1660 nm, thereby extracting the purified SRL. The single-sideband (SSB) frequency noise of the SRL is measured using the self-heterodyne method.^[32–34] The generated SRL is first directed into an acousto-optic modulator (AOM, Brimrose), which splits the beam into two paths: the 0th-order light enters a 10-km fiber delay line, while the 1st-order light (55-MHz frequency shift) passes through a polarization controller. The two beams are then recombined at a coupler and detected by a photodetector to generate a beat signal, which is recorded by a digital oscilloscope (OSC2). The recorded beat signal is processed via Hilbert transform (HT), fast Fourier transform (FFT), and compensation algorithms to retrieve the single-sideband (SSB) frequency noise power spectral density (PSD) of the SRL.^[35] Typically, the frequency noise PSD comprises $1/f$ noise at low offset frequencies and white noise at higher frequencies.^[36] In the low-frequency region, the noise power decreases with increasing offset frequency, while in the high-frequency region, it flattens out, exhibiting white-noise behavior. Assuming the observed white noise level in the high-frequency region is S_v , the laser linewidth $\Delta\nu$ can be approximated as $\Delta\nu = 2\pi S_v$.

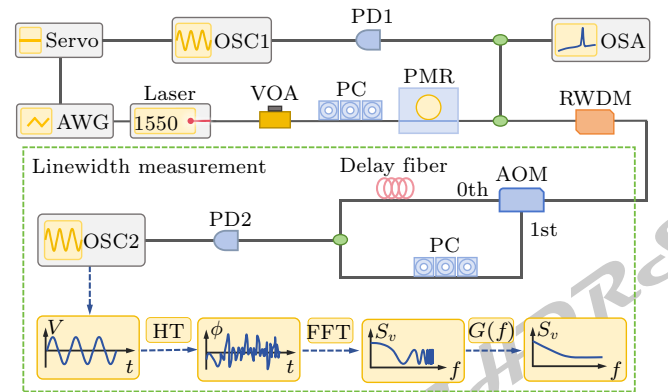


Fig. 4. Experimental setup, AWG: arbitrary waveform generator; OSC: oscilloscope; VOA: variable optical attenuator; PC: polarization controller; PMR: packaged microrod resonator; OSA: optical spectrum analyzer; RWDM: Raman wavelength division multiplexer; AOM: acousto-optic modulator; PD: photodetector; HT: Hilbert transform; FFT: fast Fourier transform; $G(f)$: compensation function.

As illustrated in Fig. 5(a), the packaged module was characterized using a Mach-Zehnder interferometer (MZI) with a 14,551-MHz FSR, yielding an intrinsic Q -factor of 1.333×10^9 for the pump mode. The optical spectrum of the SRL is shown in Fig. 5(b). The pump laser exhibited a center wavelength of 1552.644 nm, while the SRL emission was centered

at 1646.932 nm, corresponding to a Stokes shift of approximately 11.06 THz. Additionally, multiple sideband peaks with a frequency spacing of 17.2 GHz were observed near the pump laser, originating from four-wave mixing (FWM) effect.

Figure 5(c) demonstrates the dependence of the SRL output power on the pump power, with the latter controlled by a variable optical attenuator (VOA). A fit to the data reveals the threshold power of approximately 0.765 mW. To evaluate the output stability, the SRL was directed into the photodetector, which converted the optical signal into an electrical out-

put signal. This output signal was continuously monitored for 45 minutes using a data acquisition card at a sampling rate of 10 Hz. The top panel of Fig. 5(d) shows the recorded output signal, with a calculated standard deviation of 0.671 mV. The Allan variance of the laser output is also shown in the bottom panel of Fig. 5(d). The Allan variance of the SRL output signal is relatively small, exhibiting values on the order of 10^{-2} over short timescales (< 1 min), and approximately 10^{-1} over longer timescales (1 min to 10 min).

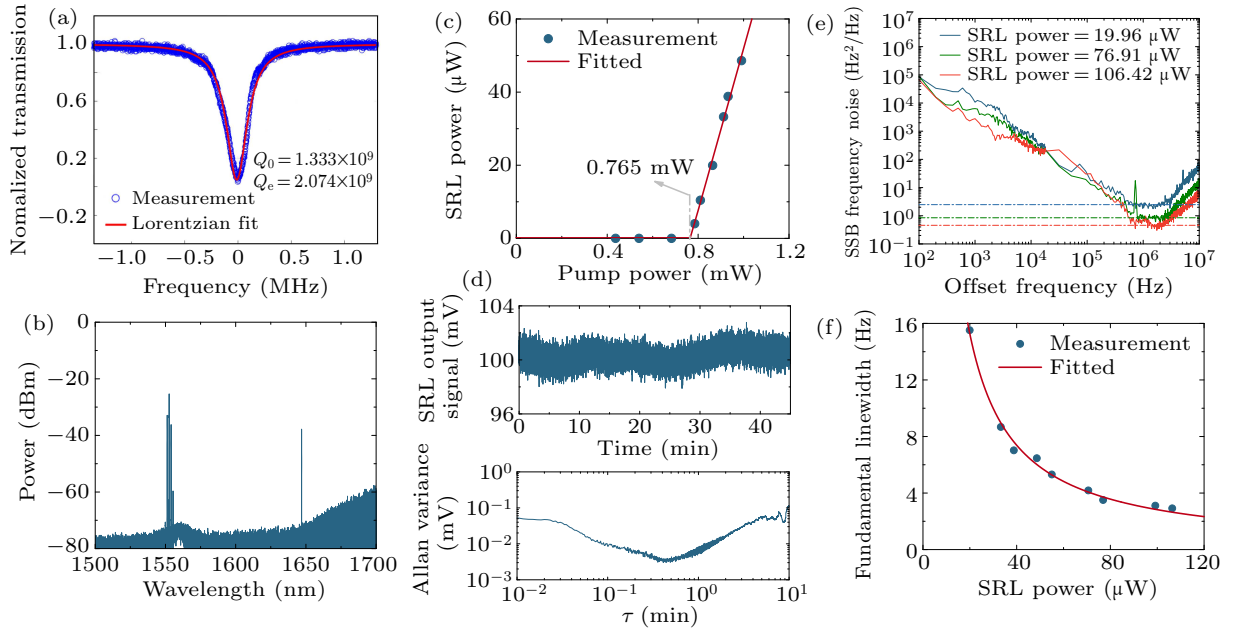


Fig. 5. Characterization of Raman laser. (a) Transmission measurement of the pump mode. (b) Optical spectra of SRL. (c) SRL power versus pump power. (d) SRL output signal (top) and Allan variance (bottom). (e) SSB frequency noise spectra of SRL at different powers. (f) Fundamental linewidth of SRL with different powers.

Additionally, we measured the frequency noise of the SRL under different output power conditions. Figure 5(e) characterizes the SSB frequency noise PSD of the SRL, where the plateau region at higher offset frequencies corresponds to the white noise. The observed white noise level exhibits reduction with increasing laser output power. When the SRL reaches its maximum output power of 106.4 μ W, the average white noise level observed is approximately 0.46 Hz^2/Hz , corresponding to a minimum laser linewidth of 2.89 Hz. Figure 5(f) illustrates the variation of the SRL linewidth as a function of output power. The fitting results demonstrate an inverse relationship between fundamental linewidth and output power, in good agreement with Eq. (1).

Thermal tuning is one of the primary methods for tuning WGM microresonator lasers due to its excellent reversibility and wide tuning range. The fundamental principle is that changes in the ambient temperature surrounding the resonator cause variations in both the cavity's physical dimensions and the refractive index of the material, resulting in a shift in the resonant wavelength. In a WGM microcavity, the temperature

dependence of the resonant wavelength can be expressed as

$$\frac{d\lambda}{dT} = \lambda_0 (\alpha + \beta), \quad (2)$$

Here, λ_0 denotes the initial resonant wavelength, α is the thermo-optic coefficient, and β represents the thermal expansion coefficient. Since silica has both a positive thermo-optic coefficient and a positive thermal expansion coefficient, the resonant modes of the silica resonator will shift toward longer wavelengths as the temperature increases.^[37,38]

During the experiment, the target temperature was set using a TEC temperature controller, forming a closed-loop feedback system with a high-sensitivity thermistor and the TEC to precisely regulate the temperature of the packaged module, as shown in Fig. 6. In the thermal tuning experiment of the SRL, the temperature of the packaged module was sequentially set to nine values: 17.6 °C, 21.2 °C, 24.4 °C, 27.1 °C, 30.4 °C, 32.8 °C, 35.5 °C, 38.1 °C, and 40.6 °C. As the temperature increased, the resonant modes of the resonator exhibited a redshift, requiring real-time adjustment of the bias voltage of the sweep signal to track the shifted resonance. The

successful reappearance of a stable Raman laser signal on the optical spectrum analyzer (OSA) confirmed the completion of laser tuning. Figure 6(a) shows the output wavelength of the pump laser tuned at different temperatures, while figure 6(b) presents the corresponding SRL excited by the pump. Experimental results show that, as the module temperature increased from 17.6 °C to 40.6 °C, the laser wavelength was continuously tuned over a range of 0.206 nm, corresponding to a wavelength–temperature tuning coefficient of 8.92 pm/°C.

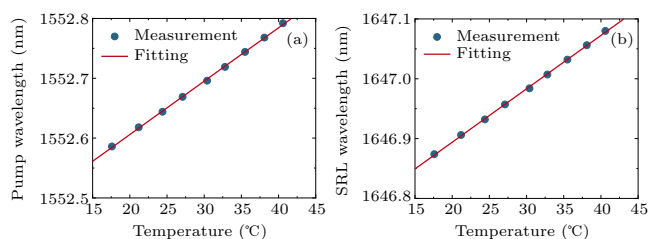


Fig. 6. Experimental results of thermal tuning: (a) pump wavelength at different temperatures, (b) variation of SRL wavelength with respect to temperature.

3. Conclusion

This study demonstrates a tunable narrow-linewidth Raman laser based on a packaged high- Q silica microrod resonator. The linewidth of this Raman laser can be narrowed to 2.89 Hz, surpassing the previous 3-Hz record linewidth demonstrated in Ref. [24]. Furthermore, the microcavity-fiber taper coupling system presented in Ref. [24] was exposed to ambient air, making it susceptible to degradation from water molecules, contaminants, and external disturbances, which can adversely affect the resonator's Q -factor and laser output stability.^[39] In contrast, we have incorporated a low-loss packaging technique. This approach consolidates the bulky fiber-coupling setup into a compact and robust enclosure for practical deployment, while simultaneously isolating the system from the external environment. The packaged module maintains a Q -factor on the order of 10^9 over a 10-day period. An integrated temperature control system stabilizes the resonator's ambient temperature to ensure stable laser output and enables wavelength tunability. The laser demonstrated high stability with an output standard deviation of 0.671 mV over 45 minutes and the continuous wavelength tuning of approximately 0.206 nm. Additionally, compared to microtoroid resonators used in Ref. [24], microrod resonators exhibit a simpler fabrication process and lower cost. Significantly, the Raman laser enables access to the underutilized U-band (1625 nm–1675 nm). This facilitates coexistence with C+L-band systems, thereby expanding optical fiber capacity without infrastructure modification. Furthermore, with its linewidth on the order of Hertz, the laser suppresses phase noise *versus* commercial DFB lasers, permitting higher order quadrature amplitude modulation for single-channel bitrate enhancement.^[40,41] The narrow-linewidth laser is promising

for high-precision gas sensing like acetylene (C_2H_2) monitoring, as its high spectral purity resolves closely spaced absorption lines.^[42,43] In conclusion, the Raman laser combines low cost, narrow linewidth, high stability, and tunability, offering application potential in diverse fields such as precision metrology, optical communications, quantum optics, and high-resolution sensing.

Acknowledgements

Project supported by the National Natural Science Foundation of China (Grant Nos. 12474372, 12474429, 62222515, and 12174438), the National Key Research and Development Program of China (Grant Nos. 2023YFB2805600 and 2023YFB2806200), the Natural Science Foundation of Beijing Municipality (Grant No. Z210004), and the Fund from the State Key Laboratory of Information Photonics and Optical Communications (Grant No. IPOC2024ZR01).

References

- [1] Hu J, Wang W, Xie Z Y, Liu C N, Li F and Yang D Q 2024 *Photon. Res.* **12** 2573
- [2] Yang Q, Li Y, Zou H, Mei J, Xu E M and Zhang Z X 2024 *Chin. Phys. B* **33** 024206
- [3] Lang X K, Jia P, Chen Y Y, Qin L, Liang L, Chen C, Wang Y B, Shan X N, Ning Y Q and Wang L J 2019 *Sci. China Inf. Sci.* **62** 19203
- [4] Duan B, Zhou H Y, Chen J H, Ma C H, Zhao X Y, Zheng X L, Wang C, Liu L and Yang D Q 2022 *Photon. Res.* **10** 2343
- [5] Chen S Y, Deng H Q, Zhang W R, Dai Y P, Wang T, Yu Q, Li C, Jiang M, Su R T and Wu J 2023 *Chin. Phys. B* **32** 074203
- [6] Duan B, Zhang X, Yu X C, Zhao Y X, Chen J H, Gao Y P, Wang C and Yang D Q 2025 *Photon. Sens.* **15** 250310
- [7] Schawlow A L and Townes C H 1958 *Phys. Rev.* **112** 1940
- [8] Wang J, Zhan T R, Huang G S, Chu P K and Mei Y F 2014 *Laser Photon. Rev.* **8** 521
- [9] Javerzac-Galy C, Kumar A, Schilling R D, Piro N, Khorasani S, Barbone M, Goykhman L, Khurgin J B, Ferrari A C and Kippenberg T J 2018 *Nano Lett.* **18** 3138
- [10] Reed J C, Zhu A Y, Zhu H, Yi F and Cubukcu E 2015 *Nano Lett.* **15** 1967
- [11] Grivas C, Li C Y, Andreakou P, Wang P F, Ding M, Brambilla G, Manna L and Lagoudakis P 2013 *Nat. Commun.* **4** 2376
- [12] Cai M, Painter O, Vahala K J and Sercel P C 2000 *Opt. Lett.* **25** 1430
- [13] Zhu S, Shi L, Xiao B W, Zhang X L and Fan X D 2018 *ACS Photon.* **5** 3794
- [14] Zhu S, Xiao B W, Jiang B, Shi L and Zhang X L 2019 *Nanophotonics* **8** 931
- [15] Tian J Y and Lin G P 2023 *J. Lightwave Technol.* **42** 2118
- [16] Spillane S M, Kippenberg T J and Vahala K J 2002 *Nature* **415** 621
- [17] Liu K K and Blumenthal D J 2024 *Conference on Lasers and Electro-Optics (CLEO)*, May 5–10, 2024, Charlotte, USA, pp. 1–2
- [18] Gundavarapu S, Brodnik G M, Puckett M, Huffman T, Bose D, Behunin R, Wu J F, Qiu T Q, Pinho C, Chauhan N, Nohava J, Rakich P T, Nelson K D, Salit M and Blumenthal D J 2019 *Nat. Photon.* **13** 60
- [19] Liu K K, Wang J W, Chauhan N, Harrington M W, Nelson K D and Blumenthal D J 2023 *Opt. Lett.* **49** 45
- [20] Qin Y C, Ding S L, Zhang M H, Wang Y N, Shi Q, Li Z X, Wen J M, Xiao M and Jiang X S 2022 *Opt. Lett.* **47** 1638
- [21] Yuan Z Q, Wang H M, Wu L, Gao M D and Vahala K J 2020 *Optica* **7** 1150
- [22] Li J, Lee H, Chen T and Vahala K J 2012 *Opt. Express* **20** 20170
- [23] Wang M, Liu C N, Zhou X, Li J C, Wang Z, Yang D Q, Yang Q F and Li B B 2025 *ACS Photon.* **12** 2318

- [24] Lu T, Yang L, Carmon T and Min B 2011 *IEEE J. Quantum Electron.* **47** 320
- [25] Liu K W, Yao S Y, Ding Y L, Wang Z H, Guo Y N, Yan J C, Wang J X, Yang C X and Bao C Y 2022 *Opt. Lett.* **47** 4295
- [26] Roos P A, Murphy S K, Meng L S, Carlsten J L, Ralph T C, White A G and Brasseur J K 2003 *Phys. Rev. A* **68** 013802
- [27] Del'Haye P, Diddams S A and Papp S B 2013 *Appl. Phys. Lett.* **102** 221119
- [28] Yang D Q, Guo Y Y, Chen W, Wu Y R, Zhai K P and Wang X 2022 *J. Lightwave Technol.* **41** 1768
- [29] Chen Y, Zhou Z H, Zou C L, Shen Z, Guo G C and Dong C H 2017 *Opt. Express* **25** 16879
- [30] Jager J B, Calvo V, Delamadeleine E, Hadji E, Noé P, Ricart T, Bucci D and Morand A 2011 *Appl. Phys. Lett.* **99** 181123
- [31] Wang H, Duan B, Wang K, Wu X Y, Gao Y P, Lu B, Yang D Q and Wang C 2023 *Nanophotonics* **12** 3757
- [32] Cui M B, Huang J G and Yang X L 2021 *Laser Optoelectron. Prog.* **58** 0900005
- [33] Yuan Z Q, Wang H M, Liu P, Li B H, Shen B Q, Gao M D, Chang L, Jin W, Feshali A, Paniccia M, Bowers J and Vahala K J 2022 *Opt. Express* **30** 25147
- [34] Chen J Q, Chen C, Sun J J, Zhang J W, Liu Z H, Qin L, Ning Y Q and Wang L J 2024 *Sensors* **24** 3656
- [35] Exter M P V, Kuppens S J M and Woerdman J P 1992 *IEEE J. Quantum Electron.* **28** 580
- [36] Domenico G D, Schilt S and Thomann P 2010 *Appl. Opt.* **49** 4801
- [37] Wu Y R, Duan B, Song J E, Liu X, Yu X C, Wang C and Yang D Q 2023 *Opt. Express* **31** 18851
- [38] Song R, Zhang X, Feng S, Liu S Y, Duan B and Yang D Q 2024 *Results Phys.* **2** 107806
- [39] Gao Y, Liu T, Wang S Y and Guo H R 2022 *Infrared Laser Eng.* **51** 20220294 (in Chinese)
- [40] Shimizu S, Takayuki K, Akira K, Takushi K, Masanori N, Koji E, Takahiro K, Masashi A, Takeshi U, Yutaka M, Tomoyuki K, Yu T and Takeshi H 2024 *J. Lightwave Technol.* **42** 1347
- [41] Xu F, Qiao Y, Zhou J, Guo M Q and Tian H P 2017 *Opt. Fiber Technol.* **34** 36
- [42] Gordon I E, Rothman L S, Hargreaves R J, et al. 2022 *J. Quant. Spectrosc. Radiat. Transf.* **277** 107949
- [43] Hodgkinson J and Tatam R P 2012 *Meas. Sci. Technol.* **24** 012004

NOT FOR AUTHOR'S
— CHINESE PHYSICS B

Chinese Physics B

Volume 34 Number 12 December 2025

Contents

TOPICAL REVIEW — Biophysical circuits: Modeling & applications in neuroscience

- 120501 Discrete neuron models and memristive neural network mapping: A comprehensive review**

Fei Yu, Xuqi Wang, Rongyao Guo, Zhijie Ying, Yan He and Qiong Zou

SPECIAL TOPIC — Biophysical circuits: Modeling & applications in neuroscience

- 120502 A sound-sensitive neuron incorporating a memristive-ion channel**

Xin-Lin Song, Ge Zhang and Fei-Fei Yang

- 120503 A new 2D Hindmarsh–Rose neuron, its circuit implementation, and its application in dynamic flexible job shops problem**

Yao Lu, Weijie Nie, Xu Wang, Xianming Wu and Qingyao Ma

- 120504 Memristive effect on a Hindmarsh–Rose neuron**

Fei Gao, Xiangcheng Yu, Yue Deng, Fang Yuan, Guangyi Wang and Tengfei Lei

- 120505 Mutual annihilation of counter-rotating spiral waves induced by electric fields**

Ying-Qi Liu, Yi-Peng Hu, Qian-Ming Ding, Ying Xie and Ya Jia

- 120506 Multi-scroll hopfield neural network excited by memristive self-synapses and its application in image encryption**

Ting He, Fei Yu, Yue Lin, Shaoqi He, Wei Yao, Shuo Cai and Jie jin

- 120701 Optimized PID neural network closed-loop control for basal ganglia network in Parkinson's disease**

Hengxi Zhang, Honghui Zhang, Shuang Liu and Lin Du

- 127301 Brain-inspired memristive pooling method for enhanced edge computing**

Wenbin Guo, Zhe Feng, Haochen Wang, Zhihao Lin, Jianxun Zou, Zuyu Xu, Yunlai Zhu, Yuehua Dai and Zuheng Wu

- 128701 Memristor-coupled dynamics and synchronization in two bi-neuron Hopfield neural networks**

Fangyuan Li, Haigang Tang, Yunzhen Zhang, Bocheng Bao, Hany Hassanin and Lianfa Bai

- 128702 Bifurcation dynamics govern sharp wave ripple generation and rhythmic transitions in hippocampal-cortical memory networks**

Xin Jiang, Jialiang Nie, Denggui Fan and Lixia Duan

(Continued on the Bookbinding Inside Back Cover)

SPECIAL TOPIC — Ultrafast physics in atomic, molecular and optical systems

- 123301 Unraveling the dynamical origin of intense fifth harmonic generation from H_2^+ in a linearly laser field**

Ling-Ling Du, Jiang-Yue Bu, Cun-Bin Chen and Xiao-Xin Zhou

COMPUTATIONAL PROGRAMS FOR PHYSICS

- 120702 MaterialsGalaxy: A platform fusing experimental and theoretical data in condensed matter physics**

Tiannian Zhu, Zhong Fang, Quansheng Wu and Hongming Weng

RAPID COMMUNICATION

- 126801 Unchanged top surface-state structures in three-dimensional topological insulator Sb_2Te_3 thin films in the presence of bottom-surface moiré potentials**

Dezhi Song, Fuyang Huang, Jun Zhang and Ye-Ping Jiang

- 127401 Crystal growth and characterization of a hole-doped iron-based superconductor $\text{Ba}(\text{Fe}_{0.875}\text{Ti}_{0.125})_2\text{As}_2$**

Yi-Li Sun, Ze-Zhong Li, Yang Li, Hong-Lin Zhou, Amit Pokhriyal, Haranath Ghosh, Shi-Liang Li and Hui-Qian Luo

- 127504 Pattern description of quantum phase transitions in the transverse antiferromagnetic Ising model with a longitudinal field**

Yun-Tong Yang, Fu-Zhou Chen and Hong-Gang Luo

GENERAL

- 120101 UHNPR: A competitive opinion information dissemination model for online social hypernetworks**

Changcai Tan, Xin Yan, Hongbin Wang, Shengxiang Gao and Zhongying Deng

- 120201 Strategy persistence-consistency and reputation promote cooperation in dual-layer networks for prisoner's dilemma games**

Qianwei Zhang, Jiaqi Liu and Leiman Fu

- 120301 Analysis of the anomalous Doppler effect from quantum theory to classical dynamics simulations**

Xinhang Xu, Jinlin Xie, Jian Liu and Wandong Liu

- 120302 Quantum algorithm for marginal Fisher analysis**

Jing Li, Yanqi Song, Sujuan Qin, Wenmin Li and Fei Gao

120303 Efficient fault-tolerant circuit for preparing quantum uniform superposition states via quantum measurement

Xiang-Qun Fu, Tian-Ci Tian, Hong-Wei Li, Jian-Hong Shi, Xiao-Liang Yang, Tan Li and Wan-Su Bao

120304 Hybrid quantum–classical multi-agent decision-making framework based on hierarchical Bayesian networks in the noisy intermediate-scale quantum era

Hao Shi, Chenghao Han, Peng Wang and Ming Zhang

120507 Energy mechanism of the first-order superradiant phase transition in cavity-BEC system with double asymmetric pump beams

Wei Qin, Dong-Chen Zheng, Jia-Ying Lin, Yuan-Hong Chen and Renyuan Liao

120508 Interval multiscale sample entropy: A novel tool for interval-valued time series complexity analysis

Ping Tang, Bao-Gen Li and Yang Wang

120509 Synchronization of a fractional-order chaotic memristive system and its application to secure image transmission

Lamia Chouchane, Hamid Hamiche, Karim Kemih, Ouerdia Megherbi and Karim Labadi

ATOMIC AND MOLECULAR PHYSICS

123101 Theoretical calculations on lifetimes of the low-lying excited states in Lu^+

Ting Liang, Min Feng, Jin Cao, Yi-Ming Wang, Ben-Quan Lu and Hong Chang

123201 Comparison of high-order harmonic generation in defect-free and defective solids with different time delays

Shujie Zhao, Yuanzuo Li, Jun Zhang and Xuefei Pan

ELECTROMAGNETISM, OPTICS, ACOUSTICS, HEAT TRANSFER, CLASSICAL MECHANICS, AND FLUID DYNAMICS

124101 Detailed simulation and characterization of double paraboloidal monocapillary for laboratory x-ray sources

Shang-Kun Shao, Tian-Yu Yuan, Cheng-Bo Li, Xing-Yi Wang, Lu Hua, Yu-Chuan Zhong, Jin-Yue Hu, Meng-Fang Chen, Xue-Peng Sun and Tian-Xi Sun

124201 Enhancement of electromagnetically induced absorption and four-wave mixing in a double two-level system

Yu-Sen Wang and Ying-Jie Du

124202 Super-resolving refractive index measurements with even coherent-state sources and parity detection

Qiang Wang, Xiaohao Yang, Fu Song and Lili Hao

124203 A tunable narrow-linewidth Raman laser based on high quality packaged microrod resonator

Cheng-Nian Liu, Min Wang, Song-Yi Liu, Bing Duan, Ying-Zhan Yan, Yu Wu, Xiao-Chong Yu, Bei-Bei Li and Da-Quan Yang

124205 Stability, bifurcation, chaotic pattern, phase portrait and exact solutions of a class of semi-linear Schrödinger equations with Kudryashov's power law self-phase modulation and multiplicative white noise based on Stratonovich's calculus

Cheng-Qiang Wang, Xiang-Qing Zhao, Yu-Lin Zhang and Zhi-Wei Lv

124206 Phase controlled single photon transport in giant atoms coupling to one-dimensional waveguide

Yan-Yan Song, Yao Zang, Yunning Lu, Zhao Liu, Xiao-San Ma and Mu-Tian Cheng

124701 Instability of nanofluid film flow under external electric field: Linear and weakly nonlinear analysis

Xinshan Li, Danting Xue, Ruigang Zhang, Quansheng Liu and Zhaodong Ding

124702 Generation of droplet group based on an external electromagnetic valve in a microfluidic chip

Dong Wang, Xiaonan Li, Jiayi Zhou, Liyu Liu and Guo Chen

124703 Quantum error mitigation based on the Z -mixed-expression of the amplitude damping channel

Ting Li, Hangming Zhang, Lingling Zheng and Fei Li

PHYSICS OF GASES, PLASMAS, AND ELECTRIC DISCHARGES

125201 Accelerating and guiding of electron beams in a cone target filled with near-critical-density plasmas

Jie-Jie Lan, Zhang-Hu Hu and You-Nian Wang

125202 Optimization of an $m = 0$ multi-loop helicon source configuration for linear plasma devices: A comparative study with Boswell and half-helix antenna designs

Yi Yu, Hao Liu, Xue-Dong Huang, Chen-Yu Xiao, Lin Nie, Guang-Yi Zhao and Min Xu

CONDENSED MATTER: STRUCTURAL, MECHANICAL, AND THERMAL PROPERTIES

126101 Intra-granular fission gas bubbles growth in crystalline U_3Si_2 : Rate theory modeling

Cong Ma, Youheng Pei, Tianyuan Xin, Dmitrii O. Kharchenko, Vasyl O. Kharchenko, Baoqin Fu, Qing Hou, Changqing Teng and Lu Wu

126102 Ion-specific hydration structures revealed by SCAN-based *ab initio* simulations

Tiancheng Liang, Liying Zhou, Yizhi Song, Xifan Wu and Limei Xu

126401 Activity waves in binary active colloids of Quincke rollers

Yuan Xie, Xiao-Yi Zhou, Qi-Ying Ni, Wen-De Tian, Kang Chen and Tian-Hui Zhang

126402 Atypical homogeneous rheology of a high-entropy metallic glass challenges standard free volume models

Guanghai Xing, Bletry Marc, Mottelet Stephane and Jichao Qiao

126701 Terahertz time-domain spectroscopy to probe laser-excited spin currents in a Co/Gd system

Fan Zhang, Bin Hong, Michel Hehn, Rongqing Zhao, Gregory Malinowski, Yong Xu, Stéphane Mangin, Jon Gorchon and Weisheng Zhao

126702 Mediated interactions between two impurities immersed in a Bose–Einstein condensate

Dong-Chen Zheng, Chun-Rong Ye, Yan-Xue Lin, Lin Wen and Renyuan Liao

CONDENSED MATTER: ELECTRONIC STRUCTURE, ELECTRICAL, MAGNETIC, AND OPTICAL PROPERTIES

127302 Sol–gel synthesis and nonvolatile resistive switching behaviors of wurtzite phase ZnO nanofilms

Zhi-Qiang Yu, Jin-Hao Jia, Mei-Lian Ou, Tang-You Sun and Zhi-Mou Xu

127303 Impact of oxide bottom electrodes on resistive switching behavior associated with oxygen vacancy dynamics in Al/ZrO₂/BE ReRAM structures

Wei Zhang, Zhen Guo, Luobin Qiu, Jun Liu and Fangren Hu

127304 A non-Hermitian approach for edge/surface states in bounded systems

Huiping Wang, Li Ren, Xiuli Zhang and Liguang Qin

127501 Resonance-assisted drastic transition in single-molecule magnets

Lei Gu, Jia Luo, Ruqian Wu and Guoping Zhao

127502 Current-driven magnetic domain wall motion in heterostructure films

Rui Fu, Jiwen Chen, Zichang Huang, Jingyi Guan, Zidong Wang and Yan Zhou

127503 NaBH₄ induces strong ferromagnetism of Bi₂Fe₄O₉ at room temperature

Chong Wang, Guorong Liu, Xiaofeng Sun, Jinyuan Ma, Tao Xian and Hua Yang

INTERDISCIPLINARY PHYSICS AND RELATED AREAS OF SCIENCE AND TECHNOLOGY

128101 Artificial synapse based on Co₃O₄ nanosheets for high-accuracy pattern recognition

Ying Li, Xiaofan Zhou, Jiajun Guo, Tong Chen, Xiaohui Zhang, Xia Xiao, Guangyu Wang, Mehran Khan Alam, Qi Zhang and Liqian Wu

- 128102 Molecular dynamics study on the effect of cooling rate on the mechanical behavior of B2-CuZr enhanced bulk-metallic glass composites**
Huahuai Shen, Kai Wang, Chenghao Chen, Jiaqing Wu, Mixun Zhu, Hongtao Zhong, Yuanzheng Yang and Xiaoling Fu
- 128401 A magnetoelectric receiving antenna with a bridge-supporting structure for ultralow-frequency wireless communication**
Boyu Xin, Qianshi Zhang, Lizhi Hu, Zishuo Fan, Jie Jiao, Chun-Gang Duan and Anran Gao
- 128402 Observation of exceptional points and realization of high sensitivity sensing in electric circuits**
Jiaxi Cai, Xinyi Wang, Xiaomin Zhang, Taoran Yue and Jijun Wang
- 128501 β -Ga₂O₃/BP heterojunction for deep ultraviolet and infrared narrowband dual-band photodetection**
Zhichao Chen, Feng Ji, Yadan Li, Yahan Wang, Xuehao Ge, Kai Jiang, Hai Zhu and Xianghu Wang
- 128703 Tumor cell directed migration based on 3D printed microfilament structure**
Dongtian Zheng, Zhikai Ye, Chuyun Wang, Lianjie Zhou, Xiyao Yao, Guoqiang Li, Guo Chen and Liyu Liu
- 128704 Molecular dynamics simulations reveal the activation mechanism of human TMEM63A induced by lysophosphatidylcholine insertion**
Zain Babar, Junaid Wahid, Xiaofei Ji, Huilin Zhao, Hua Yu and Dali Wang
- 128901 Overlapping community detection on attributed graphs via neutrosophic C-means**
Yuhan Jia, Leyan Ouyang, Qiqi Wang and Huijia Li

JUST FOR AUTHORS
— CHINESE PHYSICS B